

## Surface modified thread-based microfluidic analytical device for selective potassium analysis

Miguel M. Erenas, Ignacio de Orbe-Payá and Luis Fermin Capitan-Vallvey\*

Department of Analytical Chemistry. Campus Fuentenueva, Faculty of Sciences, 18071, University of Granada, Spain.

\* Corresponding author; email: lcapitan@ugr.es

### Abstract

This paper presents a thread-based microfluidic device ( $\mu$ TAD) that includes ionophore extraction chemistry for the optical recognition of potassium. The device is 1.5 x 1.0 cm and includes a cotton thread to transport the aqueous sample via capillary wicking to a 5 mm-long detection area, where the recognition chemistry is deposited, that reaches equilibrium in 60 s, changing its color between blue and magenta. A complete characterization of the cotton thread used as well as the sensing element has been carried out. The imaging of the  $\mu$ TAD with a digital camera and the extraction of the H coordinate of the HSV color space used as the analytical parameter make it possible to determine K(I) between  $2.4 \times 10^{-5}$  and 0.95 M with a precision better than 1.3%.

**Keywords:** Thread-based microfluidic device; Potassium determination; Ionophore-based chemistry; Digital camera;

## 1. Introduction

Optical ion recognition based on ionophores has been well known since the 1990s and has been extensively developed and applied to the determination of both organic and inorganic cations and anions.<sup>1,2</sup> The most common sensing scheme is based on the selective extraction of the target ion present in an aqueous phase to a hydrophobic membrane containing an ionophore, an event optically transduced by means of a lipophilic pH indicator due to an ion-exchange or co-extraction equilibrium triggered by the electroneutrality condition in the membrane.<sup>3</sup>

One of the drawbacks of planar film ionophore-based optical sensors (IBOS) working in equilibrium mode is the long response time –from minutes to hours depending on the analyte concentration<sup>4-6</sup>—both in flow and disposable mode, due to the need to extract the target species from the solution to the bulk of the membrane. The diffusion transport at medium/high analyte concentration and the convective mass transport at low concentration explain the response time.<sup>3,4</sup> Different strategies have been devised to reduce the response time of IBOS, with the most common ones including the ionophore chemistry in micro/nano sized spherical particles obtained by techniques such as heterogeneous polymerization,<sup>7</sup> sonic casting,<sup>8</sup> polymer swelling,<sup>9</sup> physical adsorption on the surface of microspheres<sup>10</sup> or O/W emulsion forming micelles.<sup>11</sup> The increase in the surface from the micro/nano particles and the reduction in the molecular diffusion distance enhance the mass transport and reduce the response time. The usual readout modes with particles are based on absorbance, luminescence, color, refractive index, surface plasmon resonance, microscopy and flow cytometry.<sup>3</sup> In case of quantitative optical test strips, which measure by diffuse reflectance over a membrane,<sup>12</sup> the solution is to create hydrophilic and hydrophobic zones in the membrane and to increase the porosity of the membrane. One example is the use of a hydrophilic carrier matrix such as agarose, including a buffer incorporated by emulsion with a hydrophobic liquid containing ionophore chemistry, with the emulsion then coated onto a support member.<sup>13</sup> Another example is the use of a porous carrier matrix such as a paper containing, by successive impregnations, the buffer and a homogeneous hydrophobic solution of reagents and a polymer in an organic liquid.<sup>14</sup>

The inclusion of ionophore-based chemistry in microfluidic analytical devices is an interesting option whenever an efficient interaction and a short response time are desired. Of the different microfluidic platforms –a combinable set of microfluidic unit-operations that allow for assay miniaturization within a consistent fabrication

technology<sup>15</sup>– very few examples appear in the literature. Bachas et al. propose a centrifugal microfluidics platform for K(I) determination using a planar film (2-4  $\mu\text{m}$  thickness) although they do not solve the problem of the long response time (5 minutes).<sup>16,17</sup> For their part, Hisamoto et al. use a pressure-driven laminar flow platform for alkaline ions with very short response time (8 s), performing the determination by thermal lens microscopy. They do not include the recognition chemistry in a membrane but introduce an organic solution with reagents and aqueous solution into the Y-shaped microchannel of the glass microchip with the advantages of a short diffusion distance and large interfacial area.<sup>18</sup>

Other platforms are inconvenient with regard to the inclusion of ionophore extraction recognition, as is the case with capillary platforms. Of the two main types of capillary devices, those based on paper and those based on thread, the latter is the best for implementing ionophore-based chemistry. Multifilament thread is composed of closely packed long fibers in a helical arrangement and has the property to flow liquids without external pumping in the capillary channels that form in the voids between the fibers. Its large surface allows for a thin coat with hydrophobic membranes and the movement of fluids through them.

The groups overseen by Shen<sup>19</sup> and Whitesides<sup>20</sup> were the first to propose the use of thread as a matrix to fabricate microfluidic devices ( $\mu\text{TAD}$ ) with the advantage that they do not require patterning to define the channels like paper devices do.<sup>21-23</sup> To date some examples of this application have been described, mainly in the field of diagnostics.<sup>24</sup> Most thread-based devices quantify by means of colorimetric measurements. Examples include blood typing assays,<sup>25</sup> urinalysis,<sup>19,20,26,27</sup> cancer biomarkers<sup>28</sup> and nucleic acid tests,<sup>28,29</sup> and immunochromatographic assays.<sup>30</sup> Another measurement is the chemiluminescence proposed by Lu et al.<sup>31</sup> who use a  $\mu\text{TAD}$  based on renewable flow by siphonage to analyze glucose and uric acid by covalently immobilizing oxidase enzymes on cotton thread. For their part, Sekar et al.<sup>32</sup> have presented a voltammetric device on cellulose and screen-printing pastes for different electro-active compounds.

The paper presented here presents a thread-based microfluidic colorimetric device for the simple and selective determination of K(I) based on the inclusion of an ionophore extraction membrane on cotton yarn with a very short response time.

## **EXPERIMENTAL SECTION**

### **Materials and reagents**

Potassium (1.0 M), sodium (1.0 M), magnesium (1.0 M) and calcium (1.0 M) solutions were prepared by weighing KCl, NaCl, MgCl<sub>2</sub> and CaCl<sub>2</sub>, respectively, dissolving them in water and standardizing with atomic absorption spectrometry. Then, the standards used for optimization, calibration and selectivity assays were prepared from the 1.0 M solutions described above. Tris buffers 0.2 M at pH 9.0 and 7.4 were prepared from tris(hydroxymethyl)aminomethane and HCl. Reverse osmosis type quality water (Milli-RO 12 plus Milli-Q station (Millipore, Bedford, MA, USA), conductivity 18.2 MΩ·cm) was used throughout.

The reagents used to prepare the potassium selective cocktail were polyvinyl chloride (PVC) as polymer, dibenzo18-crown-6-ether (DB18C6) as ionophore, o-nitrophenyloctylether (NPOE) as plasticizer, potassium tetrakis (4-chlorophenyl)borate (TCPB) as lipophilic salt and (1,2-benzo-7-(diethylamino)-3-(octadecanoylimino) phenoxazine (lipophilized Nile Blue) as lipophilic pH indicator dissolved in tetrahydrofuran (THF). Additionally Na<sub>2</sub>CO<sub>3</sub> was used to scour the thread. All reagents were purchased from Sigma (Sigma–Aldrich Quimica S.A., Madrid, Spain). The thread used was a commercial white cotton thread (caliber 12 and NTex 94) from Finca (Presencia Hilaturas S.A. Alzira, Valencia, Spain) measuring some 600 μm in diameter and containing 250±10 fibers (Figure S1). The thread was sewn on white ethylene-vinyl acetate (EVA) foam using a needle suitable for that purpose.

### **Instruments and Software**

The change in color of the μTAD was measured with a Canon PowerShot S5 IS digital camera (Canon Inc., Tokio, Japan). ImageJ (National Institutes of Health) software was used to analyze the region of interest (ROI) of the image along with the Color Space Converter plugin (<http://rsb.info.nih.gov/ij/plugins/color-space-converter.html>).

The size, morphology and characterization of the thread were examined by an environmental scanning electron microscope (ESEM), and energy-dispersive X-ray spectroscopy (EDX) was carried out with a SUPRA40VP Scanning Electron Microscope (Zeiss, Germany), which makes it possible to use two different detectors, a solid-state detector (SSD) and an Everhart-Thornley detector (ETD), operating at 10.0 kV with variable intensity of the electron beam. All of the studies were carried out at the Centre of Scientific Instrumentation (University of Granada).

### **Thread liquid transport study**

To investigate the liquid transport through the cotton thread, an aqueous solution of food dye Ponceau 4R (E124) 1:50 water was used. The liquid flow was recorded with a video camera working at 30 fps. Typically the required length of the thread was prepared on double-sided tape, maintained horizontally and then different volumes of ink were applied to the protruding end of the thread using a micropipette, with the data acquisition beginning at that moment. Each experiment was repeated 3 times.

### **Thread-based device preparation**

As the natural waxes present in the thread make the flow of the solutions by capillarity more difficult,<sup>33</sup> the cotton thread used as the support was scoured by boiling in an aqueous solution of 10 mg/mL Na<sub>2</sub>CO<sub>3</sub> for 5 minutes. After the treatment, the thread was washed several times with purified water until the washing water pH was near neutral (pH ≈ 6-7). Finally, the thread was dried at room temperature for 2 hours and stored in a closed container for further use.

The device consists of a 1 cm-long white thread sewn onto a piece of 1.0 x 1.5 cm white ethylene-vinyl acetate (EVA) foam to keep it stretched and allow adequate fluid movement and good image capture. Using a stitch on the side of the foam, a sampling zone 1 mm long was prepared. With two stitches typically separated by 5 mm, the thread on the top serves as the recognition zone. The thread continues on the bottom of the rubber to allow the fluid to move with a new stitch made on the top face (Figure 1).

Figure 1

To prepare the  $\mu$ TAD, 0.5  $\mu$ L of potassium sensing cocktail composed of 26.0 mg of PVC, 63.0 mg of NPOE, 0.8 mg of DB18C6, 1.3 mg of lipophilized Nile Blue and 1.1 mg of TCPB in 4.0 mL of freshly distilled THF<sup>34</sup> was added to the detection zone, then kept for 5 min at room temperature to dry and stored in the dark until use.

### **Image capture and processing**

The devices were imaged with a digital camera after reaction with samples or standards. To evaluate the color change of the ROI of the thread, some 12,000 pixels from a longitudinal section, were defined manually using the brush tool. The optimized setting conditions used to photograph the device were: macro, ISO 1600, shutter speed 1/100 s, aperture value f/3.5, focal distance 6 mm, white balance: automatic; resolution: 3264x2998; mode: super-macro. To keep all the image-gathering conditions the same, a Cube Light Box (Figure S1) was used with the camera placed in a fixed position over

the  $\mu$ TAD, which was maintained constant for all the experiments using an optical table with two LED light bulbs (3000 K) placed in a fixed arrangement with respect to the digital camera with a luminance of 165 lux measured at the stage. The captures were obtained in JPG format and processed to calculate the H coordinate of the HSV color space.

In ionophore-based optical sensors, the extension of the recognition process is measured by the degree of protonation  $1-\alpha$  of the lipophilic pH indicator<sup>34,35</sup> obtained from absorbance, fluorescence, reflectance or transfectance. In the case of color measurement by HSV color space, the H coordinate can be used directly instead of  $1-\alpha$  as we have studied elsewhere.<sup>36</sup>

### **Potassium assay**

To use the device, 10  $\mu$ L of the sample or standard aqueous solution containing between  $1.00 \times 10^{-7}$  and 0.95 M K(I) and buffered to pH 9.0 (0.01 M) with TRIS buffer was dispensed on the reception area of the  $\mu$ TAD. The sample was allowed to flow to reach the detection area and two different measurements were performed depending on the method used to determine the K(I) concentration. The first was an equilibrium-based method where the H parameter obtained at least 60 seconds after depositing the sample on the reception area is related to the logarithm of the K(I) concentration. The second is a fixed-time method, where the H value is measured 15 seconds after the sample is deposited. In both cases the concentration is calculated from the experimental Boltzmann calibration curve obtained with potassium standards.

## **RESULTS AND DISCUSSION**

Capillary platforms achieve passive liquid transport via capillary forces acting in a single capillary or in the capillaries of fibrous materials or microstructured surfaces.<sup>15</sup> Common materials used are paper, thread and cloth fabrics which, although they share capillary action, differ in the length of their fibers, interfiber bonding and porous channel structures.<sup>37</sup> Cotton fibers have a multilayered structure which consists of a primary waxy layer, a secondary wall composed of strands of cellulose and a hollow center (lumen).<sup>38,39</sup> In the case of cotton thread, both the lumen of each fiber, the gaps between the fibers constituting a yarn (intra-yarn) and the gaps between yarns constituting a thread (inter-yarn) are responsible for the capillary action by wicking the liquid into the thread.<sup>27</sup> Additionally, the whiteness of cotton thread provides a desirable

background for color-based  $\mu$ TAD. In this study we prepare a  $\mu$ TAD from commercial cotton thread composed of several yarns both for fluid transport, as a support to immobilize the detection chemistry and as a detection zone, resulting in a single-channel device.

### Thread flow behavior

The flow behavior of cotton thread, a material selected because of its good absorbency, was studied after scouring it with a  $\text{Na}_2\text{CO}_3$  solution to remove superficial noncellulosic components such as waxes and pectin by hydrolysis and oxidation, thus increasing the thread wicking wettability due to induced chemical and physical changes to the fiber surface.<sup>33</sup>

To evaluate the wicking behavior of unwaxed and as-received cotton threads, the fluid penetration distance was studied while the thread was maintained in a horizontal position. Figure 2 plots the penetration distance of fluid  $L$  as a function of time  $t$  showing that the scouring treatment improves the hydrophilic character of the cotton as well as the homogenous wicking across the length of the thread as shown by the error bars in Figure 2.<sup>26</sup>

Figure 2

To model the fluid penetration within a thread, the Washburn equation was used (equation 1) where  $\gamma$  is the interfacial tension,  $\theta$  is the contact angle between the liquid and the thread surface,  $D$  is the effective capillary diameter and  $\mu$  is the viscosity of the liquid.

$$L = \sqrt{\frac{(\gamma \cos \theta) D t}{4 \mu}} \quad \text{Equation 1}$$

The fit to the Washburn equation was obtained by fitting the experimental data with a square root function ( $L = a\sqrt{t}$ ) resulting in  $a = 0.8185$  with  $R^2 = 0.9963$  for treated thread and  $a = 0.6533$  with  $R^2 = 0.9714$  for the as-received thread. The experimental data shows some Washburn-type behavior because some factors are not considered such as the reduction in capillary force by fluid evaporation and the availability of inter-yarn gaps, which are larger than intra-yarn gaps, due to the bilobal cross-sectional geometry (Figure 2S) of the cotton thread used.<sup>37</sup>

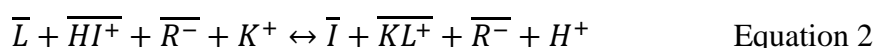
The length that different volumes of fluid advance through the thread is another important characteristic for  $\mu$ TAD design.<sup>40</sup> Figure 3 shows the exponential dependence

( $L = 1.361V^{0.717}$ ;  $R^2 = 0.9946$ ) between the volumes added ( $V$ ,  $\mu\text{l}$ ) and the distance moved through the thread ( $L$ , cm).

Figure 3

### **$\mu\text{TAD}$ preparation**

The  $\mu\text{TAD}$  for potassium is a single-channel-type device with a sampling area at the end of the thread and a detection area containing the recognition chemistry deposited with a micropipette from an organic solution. The recognition chemistry included in the  $\mu\text{TAD}$  is based on an ionophore extraction membrane<sup>3</sup> according to Equation 2:



The K(I)-selective PVC membrane works by an ion-exchange equilibrium based on dibenzo-18-crown-6-ether as ionophore (L), lipophilised Nile Blue as lipophilic pH indicator (I) and potassium tetrakis (4-chlorophenyl)borate as lipophilic salt (R). The composition of this membrane has been optimized previously for potassium determination (1L:1I:1R with 23.6 mmol/kg each).<sup>34</sup>

Usually, the sensing membranes are prepared by casting a volume of a solution of reagents in THF on a transparent support. To transfer the sensing membrane to the cotton thread we apply a volume of THF solution with a micropipette checking that it wets quickly. In response, the white changes to blue by evaporation and in response to the presence of potassium then changes its color to magenta. However, using the optimal composition of the solution as described above, the thread color is too intense to obtain precise measurements and, furthermore, as the PVC concentration is high, the samples advance along the thread slowly, increasing the response time.

To maintain the I:C:R ratio in the membrane to avoid having to change the selectivity pattern of the sensor we used 100  $\mu\text{l}$  of the serially diluted cocktail solutions with THF for  $\mu\text{TAD}$  preparation, namely 1:2, 1:3 and 1:4.

The threads covered by 1:4 diluted cocktail had a slightly blue color and a non-homogeneous distribution of the sensing membrane, which made it difficult to acquire a reliable color parameter from the ROI. Devices prepared with 1:3 and 1:2 diluted solutions had a fast response, but the range of the color coordinate H was compared when the sensor reacted with a diluted and concentrated potassium solution, it was wider for the 1:3 solution (0.62 - 0.86) than for the 1:2 solution (0.62 - 0.73). This suggests a higher sensibility for devices prepared with 1:3 solution, the concentration that was selected for the  $\mu\text{TAD}$  preparation (5.9 mmol/kg each in L, I and R) because of



the higher sensing membrane homogeneity and the wider range of analytical parameter variations.

To optimize the  $\mu$ TAD size, two different sensing area lengths were tested: 5 and 10 mm of thread. According to the relationship found between the volumes added and the distance travelled through the thread, two different volumes, 0.5  $\mu$ L and 1  $\mu$ L, were applied to prepare each detection area. To select the best device we used the criterion of the reproducibility in the response against different potassium concentrations. Four different potassium standards ( $4.00 \times 10^{-6}$  M,  $1.26 \times 10^{-4}$  M,  $4.00 \times 10^{-3}$  M and  $4.00 \times 10^{-2}$  M) were tested with 3 replicates each measuring the H coordinate. The standard deviations of H obtained from the 5 mm  $\mu$ TAD were 0.008, 0.005, 0.006 and 0.009, while for 10 mm  $\mu$ TAD they were 0.007, 0.010, 0.025 and 0.018. In conclusion, the shorter  $\mu$ TAD produces more reproducible and cheaper devices.

The morphology of the sensing membrane prepared on the cotton thread was studied by SEM evincing a non-uniform coating of the cotton fibers by the PVC sensing film. Figure 4 shows the sensing film appearing as white in the hollow spaces between the yarns and a fine white structure appears on their surface as a kind of “sensing web” that links the yarns and fills the spaces between them.

Figure 4

The EDX spectrum (Figure S3) of the areas with the white structures shows the presence of chlorine, which traces the presence of the sensing film due to lipophilic salt with PVC corroborating the white spots and fibers as sensing film. The O/C ratio increases in areas with the sensing film (0.28) compared to areas of bare cotton thread (0.15). The thin structures of the sensing film, from sub-microns to a few micron diameters thick, which appears on the cotton thread, explain the fast ion-exchange and short response time of the  $\mu$ TAD.

### **Reaction parameters**

The parameters influencing the response of the  $\mu$ TAD are pH, reaction time and potassium concentration, strictly speaking activity. To maintain the selectivity against alkaline and alkaline-earth ions, pH 9.0, adjusted with 0.01 M TRIS buffer, was used as the working pH.<sup>34</sup> Otherwise, a dependence of the reaction time with the pH is observed as shown in Figure S4 where the sensing area of the  $\mu$ TAD was recorded at different times from 300 s to 1200 s and two pH values 7.4 and 9.0. As early as 300 s the H coordinate is constant at pH 9.0, whereas for samples buffered at pH 7.4, the H

parameter is not constant even after 1140 s, meaning that the reaction has not reached equilibrium.

An in-depth study of evolution over time, performed using a video camera, of the H parameter at pH 9.0 for different potassium concentrations and using different  $\mu$ TAD shows that in the beginning, the reaction area of the protonated indicator is blue (Figure 5). When the sample is added to the  $\mu$ TAD, a very fast color change to an intermediate color between the color of the acid and the basic form of the pH indicator, independent of the potassium concentration, is observed. Figure 6 shows the evolution of the color of the  $\mu$ TAD during the first 3 s of contact with a potassium solution. That color ( $H = 0.678 \pm 0.008$ ;  $n=10$ ) corresponds to the pH indicator equilibrated at pH 9.0, a value between the blue acid form of the indicator ( $H = 0.620$ ), and the magenta base form ( $H = 0.812$ ).<sup>36</sup>

Figure 5

Figure 6

Then, the color of the thread continues to evolve due to the K(I) present in the sample, and the velocity of the process is faster as the K(I) concentration is higher in the sample. From this point, the H value of the sensor can increase or decrease from  $H=0.678$  as seen in Figure 5.

Based on this experimental behavior, we assume that the evolution of the signal can be divided into two stages. The first is very fast and the thread changes its color exclusively because of the pH of the sample (pH 9.0 buffer solution), while the second stage is due to the ion exchange process between the potassium and protons that occurs in the sensing film. The H variation because of the pH occurs very quickly (Figure 6) and can be easily observed when low K(I) concentration solutions are tested because the signal that produces the pH of the solutions is higher than the one corresponding to the potassium concentration. In that case, at the beginning the signal grows to a maximum and then decreases until equilibrium is reached.

When the signal due to the potassium solution is higher than that produced by the pH, only an increase of the H parameter is detected, although the pH process also occurs. As the pH effect over the sensor is reversible and the decrease of the signal is only observed at low concentrations, we can assume that this process does not affect the ion exchange process. In short, 60 s is enough to reach the equilibrium in the  $\mu$ TAD.

The ion-exchange process (Equation 2) and the extension of the reaction depend on the exchange constant ( $K_{Exch}$ ), which in turn depend on the concentration of the reagents,

pH and potassium concentration, charge of the analyte and stoichiometry of the reaction defined as follows (Equation 3):

$$K_{exch} = \frac{1}{a_{I^{v+}}} \left( \frac{a_{H^+} \alpha}{1 - \alpha} \right)^v \frac{C_R - (1 - \alpha)C_C}{v \left( C_L - \frac{p}{v} (C_R - (1 - \alpha)C_C) \right)^p} \quad \text{Equation 3}$$

where  $C_L$ ,  $C_C$  and  $C_R$  are the analytical concentrations of the ionophore, lipophilic pH indicator and lipophilic salt, respectively, and  $p$  is the stoichiometric factor for the complex formed,  $v$  is the analyte charge and  $1 - \alpha$ <sup>3</sup> is the degree of protonation of the pH indicator. The  $K_{exch}$  value calculated from the H experimental data set<sup>36</sup> was  $3.78 \times 10^{-7}$ , a value similar to  $K_{exch}$  for the same system obtained from absorbance measurements  $2.57 \times 10^{-7}$  and  $9.35 \times 10^{-8}$  obtained from H values.<sup>36</sup>

### Calibration and analytical parameters

The H readout obtained after equilibration (60 s) of the  $\mu$ TAD with potassium is used directly as the analytical parameter due to its small device-to-device variation (less than 1%). To obtain the calibration function, fourteen potassium standards from  $1.00 \times 10^{-7}$  to 1.00 M and three replicates per solution were analyzed with a new  $\mu$ -TAD each time, thus obtaining a robust H data set that was used to obtain the calibration function in Figure 7.

The response of the  $\mu$ -TAD has the usual sigmoidal shape of ionophore-based optical sensors, adjusting the data set to a Boltzmann equation<sup>36</sup> (Table 1) with  $R^2 = 0.9909$ . The limit of detection (LOD) was calculated by adding the standard deviation of the blank six times.<sup>3</sup> The blank was obtained from the H value of the  $\mu$ TAD reacted with 10  $\mu$ L of the pH 9.0 buffer solution. The LOD calculated with this method was  $2.4 \times 10^{-5}$  M (0.94 mg/l), and then the dynamic range went from  $2.4 \times 10^{-5}$  to 0.1 M. The LOD obtained is a little worse than that obtained using the same chemistry disposed in a planar membrane measuring color with the HSV ( $4.5 \times 10^{-6}$  M)<sup>36</sup> or RGB ( $6.58 \times 10^{-6}$  M)<sup>41</sup> space due to the different criteria used to define the LOD.

The precision of the procedure using different devices was calculated at three potassium concentrations ( $1.26 \times 10^{-4}$ ,  $1.26 \times 10^{-3}$ ,  $4.00 \times 10^{-2}$  M) using 10 replicates each, obtaining a mean relative standard deviation of 1.34% (Table 1). This means a better precision compared to other thread-based procedures: Mao et al.<sup>28</sup> found a 9.3% RSD for the biomarker squamous cell carcinoma antigen test; the procedure for DNA detection

described by Du et al.<sup>29</sup> has a precision of 9.8%; Lu et al.<sup>31</sup> found precisions around 5% in their enzymatic test for hydrogen peroxide and related analytes based on chemiluminescence measurement. The precision figures found here can be ascribed to the simple device used and the use of the H coordinate.<sup>36</sup>

The selectivity of the sensing system for potassium disposed on thread against alkaline and alkaline-earth ions was checked using the separated solutions method.<sup>42,43</sup> The  $1-\alpha$  value needed for this calculation was obtained from the H coordinate as described elsewhere<sup>36</sup> (see ESI and Figure S5 for selectivity calculation). Table 1 shows the  $k_{ij}^{\text{opt}}$  from each potassium-interference couple concluding that the  $\mu$ -TAD developed is very selective for potassium even in the presence of a high concentration of other alkaline and earth-alkaline ions.

Table 1

To reduce the analysis time, we studied the feasibility of the calibration measuring the H value of the  $\mu$ TAD at different times, namely at 5, 15, 25 and 40 s. From 15 s onwards it is possible to obtain sigmoidal calibration functions with a small increase in the dynamic range, reaching the maximum in equilibrium conditions at 60 s. Figure S6 shows the calibration curve with the error bars for 15 s and a LOD of  $1.2 \times 10^{-4}$  M and upper limit of the dynamic range of 0.2 M. Times lower than 15 s have a very short dynamic range because of the thread color changes, due to the pH of the sample as discussed above. The measurement during the kinetic stage of the recognition process provides an approximation of the potassium concentration in a very short time.

### **$\mu$ TAD lifetime**

The lifetime of the  $\mu$ TADs was studied with a set of devices in two storage conditions: a first group of  $\mu$ TADs was preserved in a black-painted desiccator at room temperature and a second in a similar desiccator under nitrogen atmosphere. The lifetime was studied at 27 days by checking the responses of three different  $\mu$ TADs against a  $1.25 \times 10^{-3}$  M potassium solution. The results presented in Figure 7 show that the  $\mu$ TAD has a low lifetime of some 3 days even in a nitrogen atmosphere. The very thin wire morphology of the sensing film adhered to the cellulosic material is probably the cause of the low stability.

Figure 7

### **Application of the method**

The proposed method was applied to the determination of potassium in different mineral waters. The representative measurements using the  $\mu$ TAD are outlined in Table 2 and compared to the atomic absorption spectrometry method, which is used as a reference method. This table also includes the mean values in triplicate samples with their associated standard deviation and the probability value ( $P_{\text{val}}$ ) of the test used to compare the results from both methods, with no significant statistical differences at a confidence level of 95%.

Table 2

## **Conclusion**

We have prepared a  $\mu$ TAD-type single-channel device based on commercial hydrophilic cotton thread for fluid transport, a support to immobilize the detection chemistry and as the detection zone. The use of diluted cocktails containing ionophore extraction-based sensing chemistry solves the problem of the wet thread impregnated with a hydrophobic membrane containing the detection chemistry that hinders the use of these recognition chemistries in microfluidic systems operated by capillarity. This allows for very short equilibration times, as low as 60 s, which can be reduced to 15 s by doing the measurement during the kinetic stage of the process. As usual with this type of recognition chemistry, the dynamic range of the procedure is ample, some four orders of magnitude in this case.

The use of commercial imaging devices such as digital cameras to obtain analytical information makes it possible to easily acquire color information from thread which, when combined with the use of tonal coordinate (H) of the HSV color space, results in a procedure with very good precision. This ameliorates one of the disadvantages of thread-based procedures: their low precision. These thread-based devices have potential applications in environmental monitoring and medical diagnostics, among other areas, with the advantages of easy manipulation, chemical information acquisition using smartphones primarily and a low fabrication cost (an estimated cost of 1.7 cents per unit in this case). Other applications using thread as the support for microfluidic devices, along with the search for new strategies to improve their lifetime and reusability, are now under investigation and will be the subject of future work.

## **Acknowledgements**

This work was supported by project CTQ2013-44545-R from the *Ministerio de Economía y Competitividad* (Spain) and *Junta de Andalucía (Proyecto de Excelencia*

P10-FQM-5974. These projects were partially supported by European Regional Development Funds (ERDF).

## References

1. Bühlmann, P.; Pretsch, E.; Bakker, E. Carrier-Based ion-Selective Electrodes and bulk Optodes. 2.-Ionophores for Potentiometric and optical Sensors. *Chem. Rev.* **1998**, *98*, 1953-1687.
2. Spichiger-Keller, U. E. Optical Sensors, Optodes. In *Chemical Sensors and Biosensors for Medical and Biological Applications*, 1 ed.; Wiley-VCH: Weinheim, 1998; pp 259-319.
3. Mistberger, G.; Crespo, G. A.; Bakker, E. Ionophore-based optical sensors. *Annu. Rev. Anal. Chem.* **2014**, *7*, 483-512.
4. Lerchi, M.; Bakker, E.; Rusterholz, B.; Simon, W. Lead-Selective Bulk Optodes Based on Neutral Ionophores with Subnanomolar Detection Limits. *Anal. Chem.* **1992**, *64*, 1534-1540.
5. Lerchi, M.; Reitter, E.; Simon, W.; Pretsch, E.; Chowdhury, A.; Kamata, S. Bulk Optodes Based on Neutral Dithiocarbamate Ionophores with High Selectivity and Sensitivity for Silver and Mercury Cations. *Anal. Chem.* **1994**, *66*, 1713-1717.
6. Capitan-Vallvey, L. F.; Arroyo-Guerrero, E.; Fernandez-Ramos, M. D.; Santoyo-Gonzalez, F. Disposable receptor-based optical sensor for nitrate. *Anal. Chem.* **2005**, *77* (14), 4459-4466.
7. Xu, C.; Wygladacz, K.; Qin, Y.; Retter, R.; Bell, M.; Bakker, E. Microsphere optical ion sensors based on doped silica gel templates. *Anal. Chim. Acta* **2005**, *537* (1-2), 135-143.
8. Peper, S.; Bakker, E. Fluorescent Ion-Sensing Microspheres for Multiplexed Chemical Analysis of Clinical and Biological Samples. *Sensors Update* **2003**, *13* (1), 83-104.
9. Shakhsher, Z. M.; Odeh, I.; Jabr, S.; Rudolf Seitz, W. An Optical Chemical Sensor Based on Swellable Dicarboxylate Functionalized Polymer Microspheres for pH, Copper and Calcium Determination. *Microchim. Acta* **2004**, *144* (1-3), 147-153.
10. Xie, X.; Crespo, G. A.; Zhai, J.; Szilagyi, I.; Bakker, E. Potassium-selective optical microsensors based on surface modified polystyrene microspheres. *Chem. Commun.* **2014**, *50* (35), 4592-4595.
11. Zhai, J.; Xie, X.; Bakker, E. Ionophore-based ion-exchange emulsions as novel class of complexometric titration reagents. *Chem. Commun.* **2014**, *50* (84), 12659-12661.

12. Capitan-Vallvey, L. F.; Fernandez-Ramos, M. D. Solid-phase spectrometric assays. In *Integrated Analytical Systems*, Alegret, S., Ed.; Elsevier Science B.V: Amsterdam, 2003; Vol. XXXIX, pp 81-159.
13. Charlton, S. C.; Hemmes, P.; Lau, A. L. Y. Ion test means having a hydrophilic carrier matrix. US 4,649,123, 1987.
14. Gantzer, M. L.; Hemmes, P. R.; Wong, D. Ion test having a porous carrier matrix. US 4,670,218, 1987.
15. Mark, D.; Haeberle, S.; Roth, G.; von Stetten, F.; Zengerle, R. Microfluidic lab-on-a-chip platforms: requirements, characteristics and applications. *Chem. Soc. Rev.* **2010**, *39* (3), 1153-1182.
16. Badr, I. H. A.; Johnson, R. D.; Madou, M. J.; Bachas, L. G. Fluorescent Ion-Selective Optode Membranes Incorporated onto a Centrifugal Microfluidics Platform. *Anal. Chem.* **2002**, *74* (21), 5569-5575.
17. Johnson, R. D.; Badr, I. H. A.; Barrett, G.; Lai, S.; Lu, Y.; Madou, M. J.; Bachas, L. G. Development of a Fully Integrated Analysis System for Ions Based on Ion-Selective Optodes and Centrifugal Microfluidics. *Anal. Chem.* **2001**, *73* (16), 3940-3946.
18. Hisamoto, H.; Horiuchi, T.; Tokeshi, M.; Hibara, A.; Kitamori, T. On-Chip Integration of Neutral Ionophore-Based Ion Pair Extraction Reaction. *Anal. Chem.* **2001**, *73* (6), 1382-1386.
19. Li, X.; Tian, J.; Shen, W. Thread as a Versatile Material for Low-Cost Microfluidic Diagnostics. *ACS Appl. Mater. Interfaces* **2010**, *2* (1), 1-6.
20. Reches, M.; Mirica, K. A.; Dasgupta, R.; Dickey, M. D.; Butte, M. J.; Whitesides, G. M. Thread as a Matrix for Biomedical Assays. *ACS Appl. Mater. Interfaces* **2010**, *2* (6), 1722-1728.
21. Cate, D. M.; Adkins, J. A.; Mettakoonpitak, J.; Henry, C. S. Recent Developments in Paper-Based Microfluidic Devices. *Anal. Chem.* **2014**, *87* (1), 19-41.
22. Hu, J.; Wang, S.; Wang, L.; Li, F.; Pingguan-Murphy, B.; Lu, T. J.; Xu, F. Advances in paper-based point-of-care diagnostics. *Biosensors Bioelectron.* **2014**, *54* (0), 585-597.
23. Santhiago, M.; Nery, E. W.; Santos, G. P.; Kubota, L. T. Microfluidic paper-based devices for bioanalytical applications. *Bioanalysis* **2014**, *6* (1), 89-106.
24. Nilghaz, A.; Ballerini, D. R.; Shen, W. Exploration of microfluidic devices based on multi-filament threads and textiles: A review. *Biomicrofluidics* **2013**, *7* (5), 51501.
25. Nilghaz, A.; Zhang, L.; Li, M.; Ballerini, D. R.; Shen, W. Understanding Thread Properties for Red Blood Cell Antigen Assays: Weak ABO Blood Typing. *ACS Appl. Mater. Interfaces* **2014**, *6* (24), 22209-22215.

26. Nilghaz, A.; Ballerini, D. R.; Fang, X. Y.; Shen, W. Semiquantitative analysis on microfluidic thread-based analytical devices by ruler. *Sens. Actuators B* **2014**, *191*, 586-594.
27. Banerjee, S. S.; Roychowdhury, A.; Taneja, N.; Janrao, R.; Khandare, J.; Paul, D. Chemical synthesis and sensing in inexpensive thread-based microdevices. *Sens. Actuators B* **2013**, *186*, 439-445.
28. Mao, X.; Du, T. E.; Wang, Y.; Meng, L. Disposable dry-reagent cotton thread-based point-of-care diagnosis devices for protein and nucleic acid test. *Biosens. Bioelectron.* **2015**, *65*, 390-396.
29. Du, T. E.; Wang, Y.; Zhang, Y.; Zhang, T.; Mao, X. A novel adenosine-based molecular beacon probe for room temperature nucleic acid rapid detection in cotton thread device. *Anal. Chim. Acta* **2015**, *861* (0), 69-73.
30. Zhou, G.; Mao, X.; Juncker, D. Immunochromatographic Assay on Thread. *Anal. Chem.* **2012**, *84* (18), 7736-7743.
31. Lu, F.; Mao, Q.; Wu, R.; Zhang, S.; Du, J.; Lv, J. A siphonage flow and thread-based low-cost platform enables quantitative and sensitive assays. *Lab Chip* **2014**, *15* (2), 495-503.
32. Sekar, N. C.; Mousavi Shaegh, S. A.; Ng, S. H.; Ge, L.; Tan, S. N. Simple thick-film thread-based voltammetric sensors. *Electrochem. Commun.* **2014**, *46*, 128-131.
33. Nilghaz, A.; Wicaksono, D. H. B.; Gustiono, D.; Abdul Majid, F. A.; Supriyanto, E.; Abdul Kadir, M. R. Flexible microfluidic cloth-based analytical devices using a low-cost wax patterning technique. *Lab Chip* **2012**, *12* (1), 209-218.
34. Capitan-Vallvey, L. F.; Fernandez Ramos, M. D.; Al Natsheh, M. A disposable single-use optical sensor for potassium determination based on neutral ionophore. *Sens. Actuators B* **2003**, *88* (2), 217-222.
35. Bakker, E.; Bühlmann, P.; Pretsch, E. Carrier-Based Ion-Selective Electrodes and Bulk Optodes. 1. General Characteristics. *Chem Rev.* **1997**, *97*, 3083-3132.
36. Cantrell, K.; Erenas, M. M.; Orbe-Paya, I.; Capitan-Vallvey, L. F. Use of the Hue Parameter of the Hue, Saturation, Value Color Space as a Quantitative Analytical Parameter for Bitonal Optical Sensors. *Anal. Chem.* **2010**, *82* (2), 531-542.
37. Ballerini, D. R.; Li, X.; Shen, W. Flow control concepts for thread-based microfluidic devices. *Biomicrofluidics* **2011**, *5* (1), 014105-1-014105/13.
38. Dochia, M.; Sirghie, C.; Kozłowski, R. M.; Roskwitalski, Z. 2 - Cotton fibres. In *Handbook of Natural Fibres* Woodhead Publishing Series in Textiles, 1 ed.; Kozłowski, R. M., Ed.; Woodhead Publishing: 2012; pp 11-23.



39. Hsieh, Y. L. Chemical structure and properties of cotton. In *Cotton Woodhead Publishing Series in Textiles*, Gordon, S., Hsieh, Y. L., Eds.; Woodhead Publishing: 2007; pp 3-34.
40. Safavieh, R.; Zhou, G. Z.; Juncker, D. Microfluidics made of yarns and knots: from fundamental properties to simple networks and operations. *Lab Chip* **2011**, *11* (15), 2618-2624.
41. Lapresta-Fernandez, A.; Capitan-Vallvey, L. F. Scanometric potassium determination with ionophore-based disposable sensors. *Sens. Actuators B* **2008**, *134* (2), 694-701.
42. Bakker, E.; Simon, W. Selectivity of Ion-Sensitive Bulk Optodes. *Anal. Chem.* **1992**, *64*, 1805-1812.
43. IUPAC Recommendations for Nomenclature of Ion-Selective Electrodes. *Pure Appl. Chem.* **1976**, *48*, 127.

Table 1. Analytical parameters and calibration function of the potassium  $\mu$ -TAD

Analytical Parameters			
<b>Boltzmann equation</b>		<b>Intermembrane precision (n=10)</b>	
$H = \frac{A_1 - A_2}{1 + e^{\frac{\log[K(I)] - x_0}{dx}}} + A_2$			
<b>A<sub>1</sub></b>	<b>0.62</b>	<b>1.26x10<sup>-4</sup> M</b>	<b>1.57%</b>
<b>A<sub>2</sub></b>	<b>0.85</b>	<b>1.26x10<sup>-3</sup> M</b>	<b>1.19%</b>
<b>x<sub>0</sub></b>	<b>-2.55</b>	<b>4.00x10<sup>-2</sup> M</b>	<b>1.25%</b>
<b>dx</b>	<b>0.50</b>	<b>Selectivity</b>	
<b>R<sup>2</sup></b>	<b>0.9909</b>	<b>Log K<sub>Na(I)-K(I)}<sup>opt</sup></sub></b>	<b>-2.59</b>
<b>Limit of detection</b>	<b>2.4x10<sup>-5</sup> M</b>	<b>Log K<sub>Ca(II)-K(I)}<sup>opt</sup></sub></b>	<b>-3.54</b>
<b>Dynamic range</b>	<b>2.4x10<sup>-5</sup> - 0.95 M</b>	<b>Log K<sub>Mg(II)-K(I)}<sup>opt</sup></sub></b>	<b>-8.10</b>

Table 2. Determination of potassium in different water samples using the proposed and reference procedures

Sample	AAS		$\mu$ -TAD 15 s			$\mu$ -TAD 60 s		
	K(I) (mM)	s <sup>(1)</sup>	K(I) (mM)	s <sup>(1)</sup>	P <sub>val</sub> (%)	K(I) (mM)	s <sup>(1)</sup>	P <sub>val</sub> (%)
Mineral water (Lanjarón)	1.31	0.04	----	----	—	1.35	0.11	60.6
Tap water (Granada)	1.21	0.05	1.43	1.07	29.9	1.30	0.75	84.8
Mineral water (Solán de Cabras)	1.25	0.01	1.43	1.06	17.8	1.22	1.03	18.8

(1) Standard deviation from three replicates.

## Figure Captions

**Figure 1.**  $\mu$ -TAD for potassium. A) Diagram of  $\mu$ TAD with dimensions. B) Picture of  $\mu$ -TAD with two sensing areas for redundancy.

**Figure 2.** Evolution of fluid penetration in unwaxed (a) and as-received (b) cotton from data obtained from a video. 10-cm long threads wicked with 50  $\mu$ L dye solution. Solid lines fit the experimental data to a Washburn equation.

**Figure 3.** Distance advanced by different volumes (from 0.5 to 15  $\mu$ l) of dye solution when added to the end of a 10 cm-long scoured thread.

**Figure 4.** Image of the cotton thread coated with PVC sensing film obtained from a SUPRA40VP Scanning Electron Microscope. A) Image of a cross-sectional view of thread showing the lumen showing the inside of some yarn (black holes) and non-uniform coating of the film as a fine white structure linking the yarns. B) Longitudinal section of the thread with sensing film.

**Figure 5.** Evolution of H parameter during the reaction of the  $\mu$ TAD with different potassium concentrations. There is a common H value at 3 s thanks to the reversible and fast pH reaction due to the pH of the sample followed by the ionophore extraction of potassium to the membrane.

**Figure 6.** Fast color change of the  $\mu$ TAD due to the pH of the sample. This reaction occurs regardless of the K(I) concentration.

**Figure 7.** Calibration function for potassium (14 K(I) standards solution, n=3). The blue line represents the fit of the experimental data to a sigmoidal equation and the red line is the confidence limit of the regression.

**Figure 8.** Lifetime of the  $\mu$ TAD device for potassium determination tested with  $1.25 \times 10^{-3}$  M potassium. Blue dots: preserved in black-painted desiccator at room temperature. Red dots: preserved in black-painted desiccator at room temperature under nitrogen.

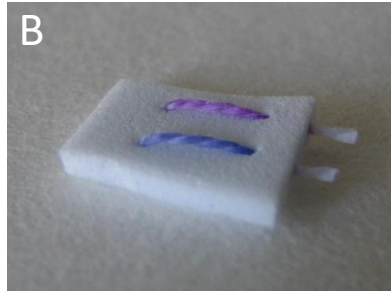
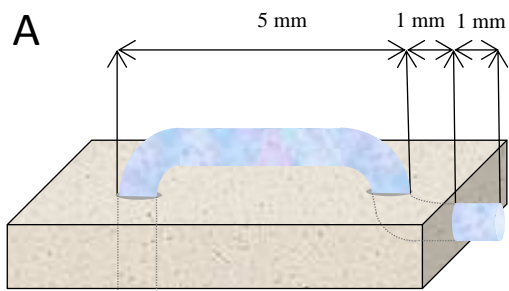


Figure 1

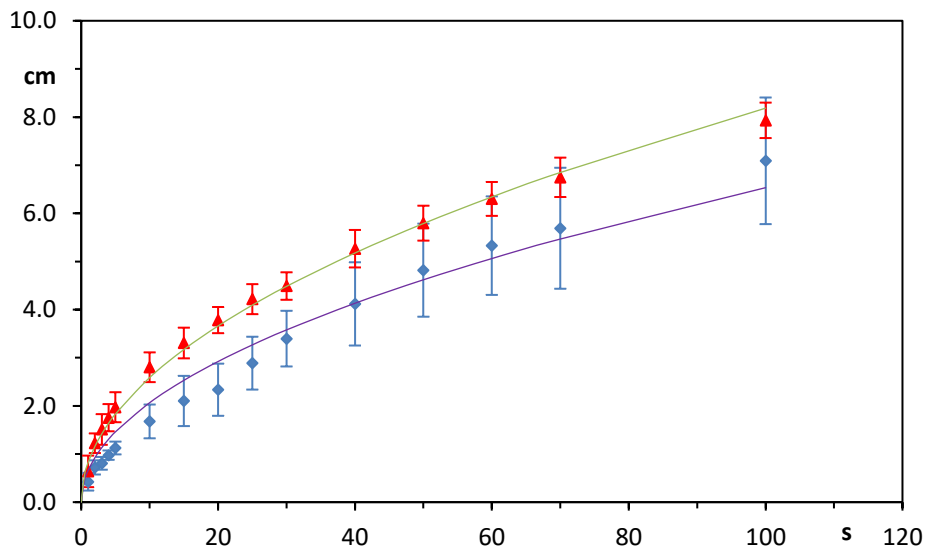


Figure 2

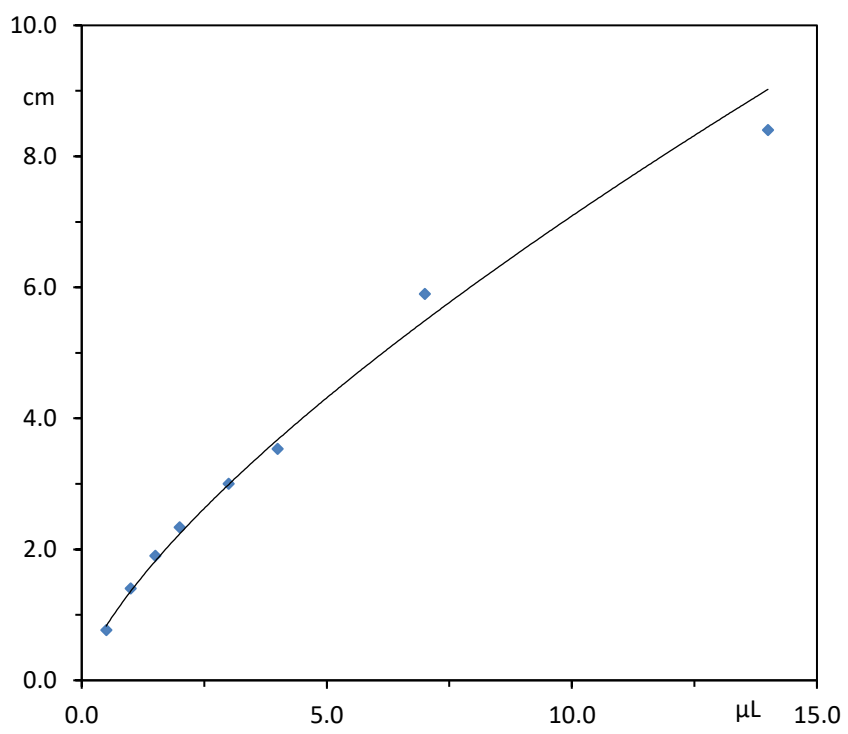


Figure 3

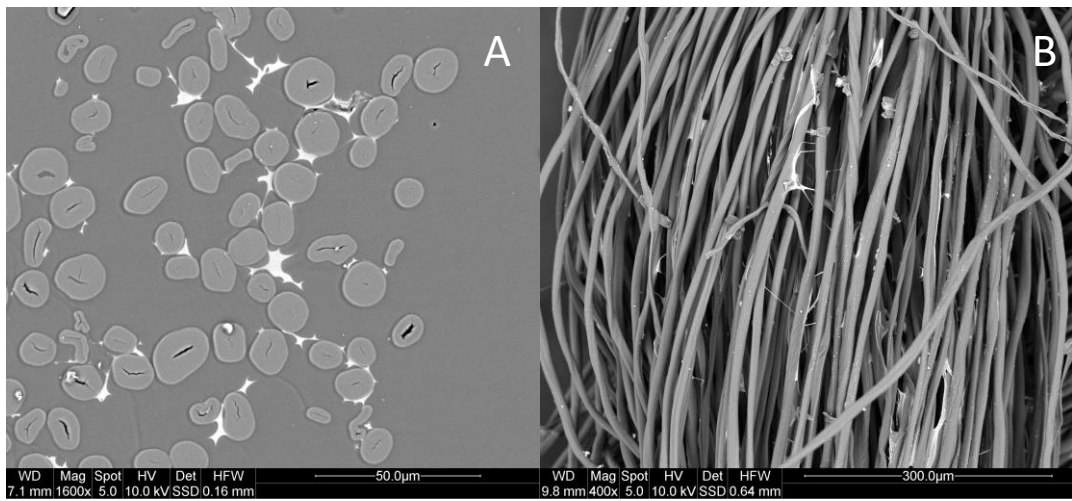


Figure 4



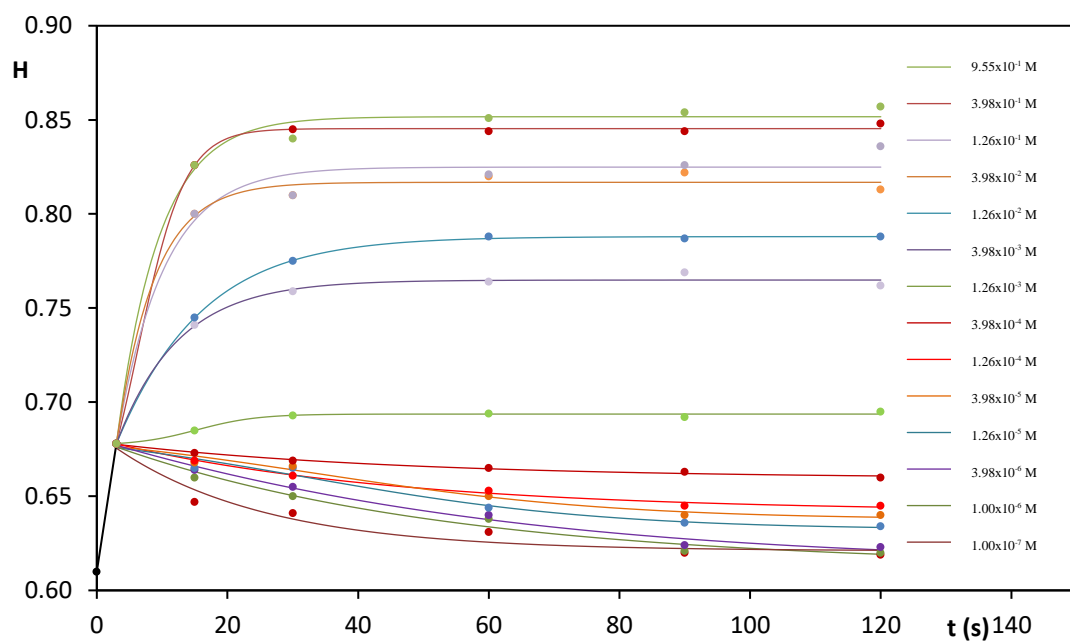


Figure 5

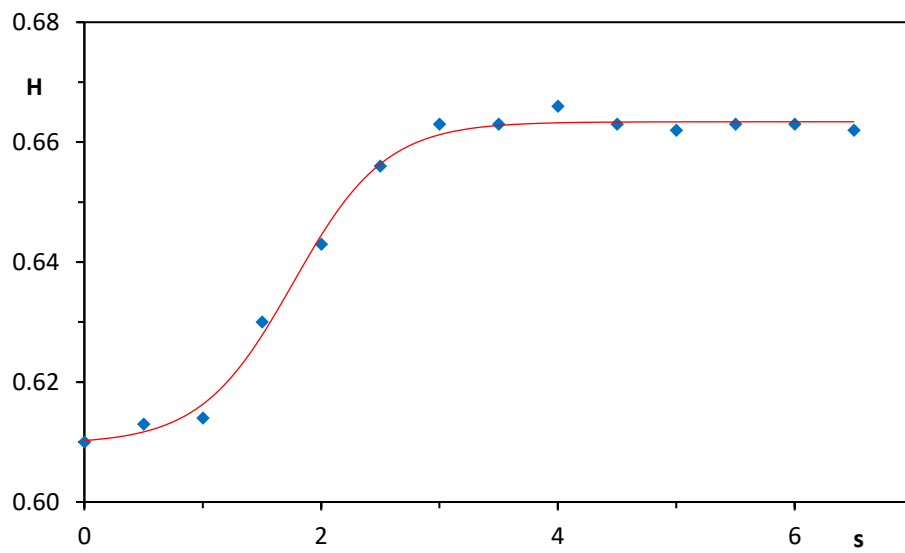


Figure 6

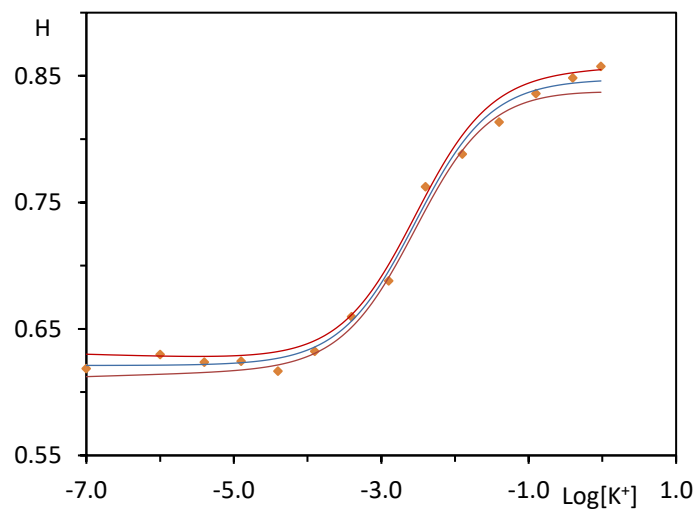


Figure 7

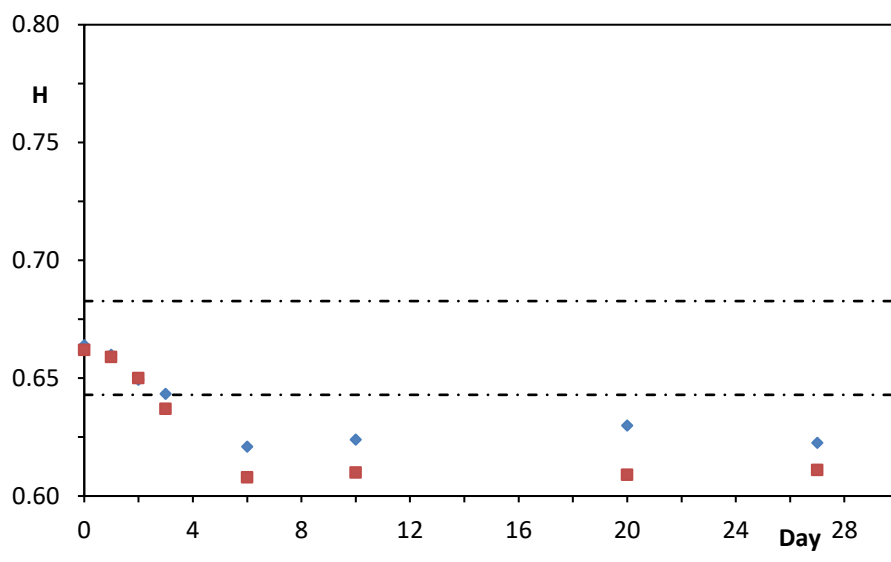


Figure 8